

超新星遗迹粒子加速与辐射 形态

方军

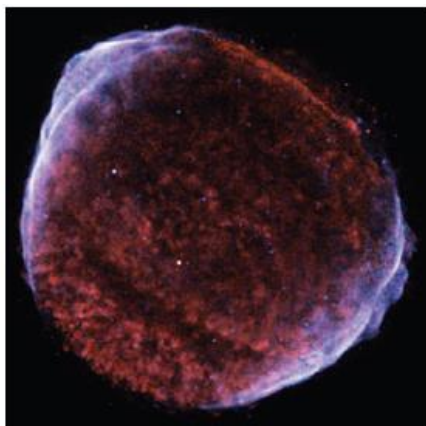
云南大学 天文学系

2017 昆明

一、超新星遗迹 (壳型 shell-type) 研究与观测背景

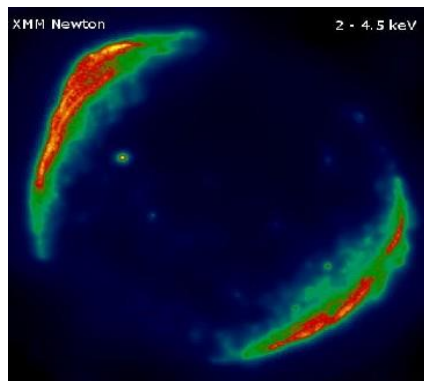
银河系宇宙线粒子 ($<10^{15}\text{eV}$) 起源地。(能损、能谱)

非热辐射源, 射电、X-ray、伽玛射线。

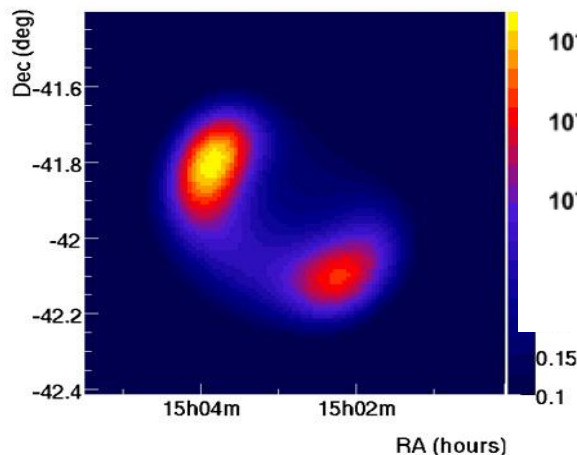


Chandra

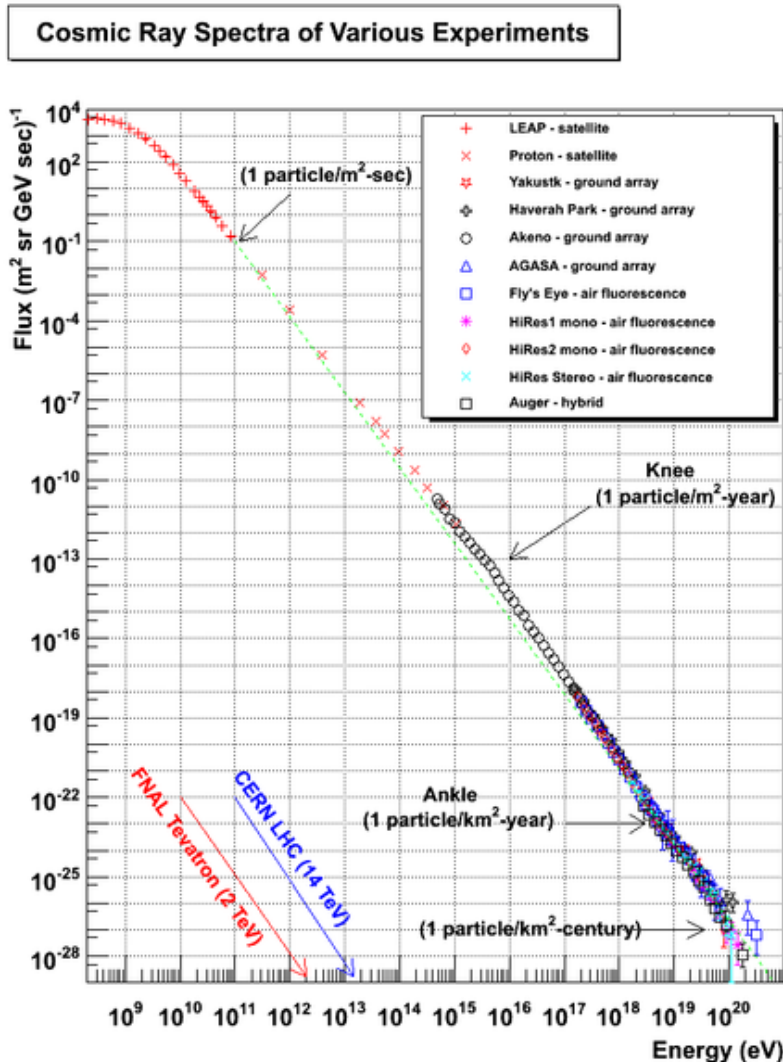
SN 1006



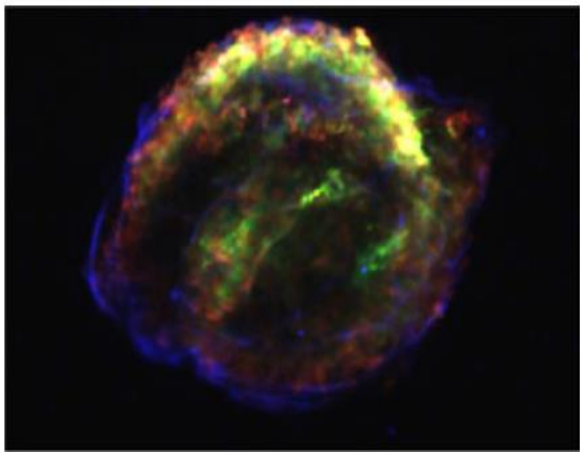
XMM-Newton



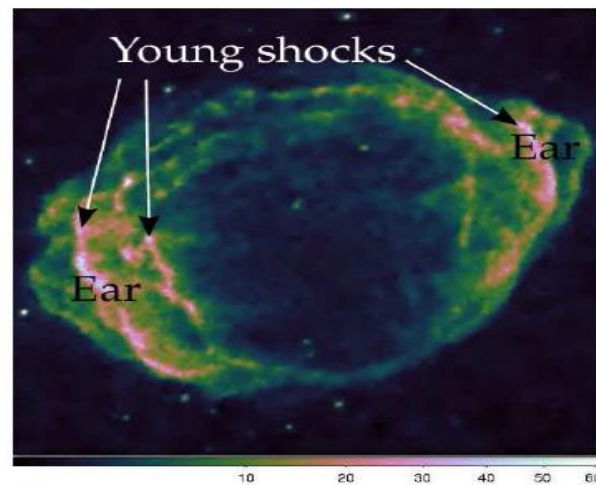
SNR 粒子加速与辐射形成



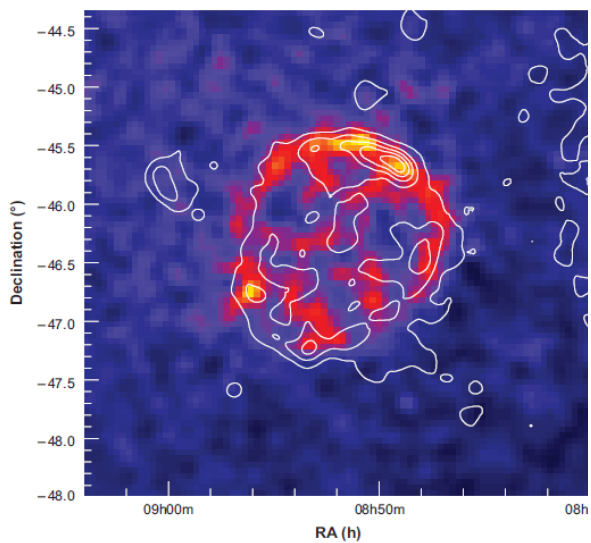
HESS



Kepler's
SNR

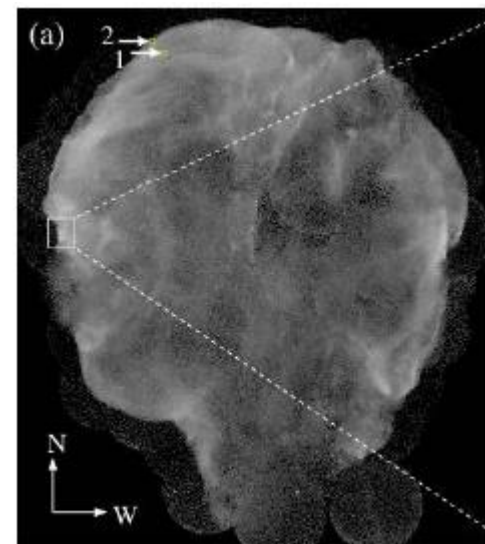
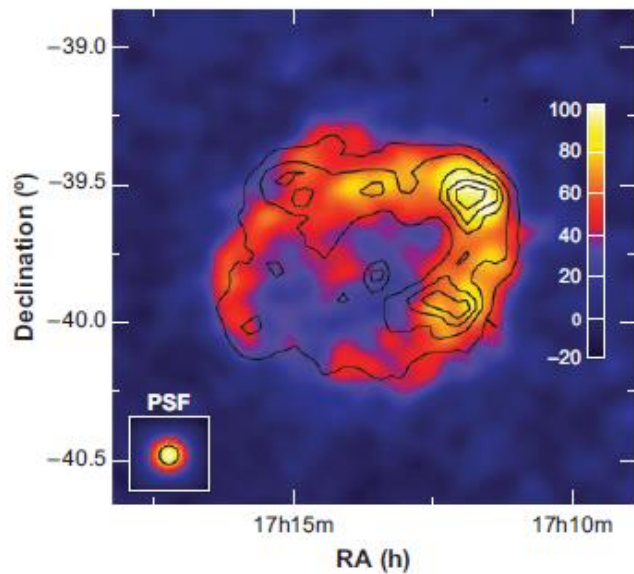


G1.9+0.3



RX J0852.0-4622

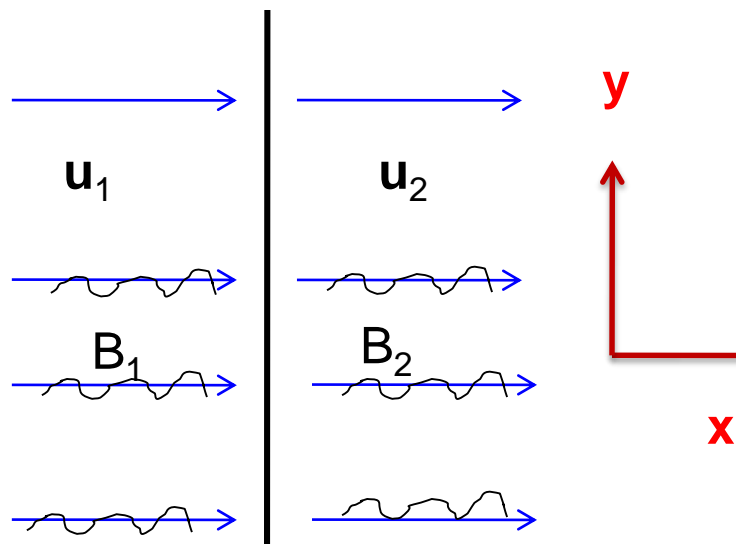
a



Cygnus loop

粒子加速

(1) 扩散激波加速 (shock diffusive acceleration)



in the shock rest frame

激波结构，试验粒子近似下

$$v(x) = \begin{cases} v_1 & \text{for } x < 0 \\ v_2 = v_1/r & \text{for } x > 0 \end{cases}$$

$$r = \frac{\rho_2}{\rho_1} = \frac{v_1}{v_2}$$

强激波近似下，

$$r = \frac{\gamma_g + 1}{\gamma_g - 1}$$

$$\frac{\partial f}{\partial t} = \nabla \cdot (D \nabla f) - \nabla \cdot (f \vec{v}) + \frac{1}{3} \frac{\partial (f p)}{\partial p} \nabla \cdot \vec{v}$$

$D(r, p)$ 为扩散系数。

一维稳态情况下，

$$\frac{\partial}{\partial x} \left[v f(x, p) - D(x, p) \frac{\partial f(x, p)}{\partial x} \right] = \frac{1}{3} \frac{\partial v}{\partial x} \frac{\partial}{\partial p} [p f(x, p)]$$

考虑边界条件

$$f(x = -\infty, p) = f_1(p), \text{ and } f(x = +\infty, p) = f_2(p)$$

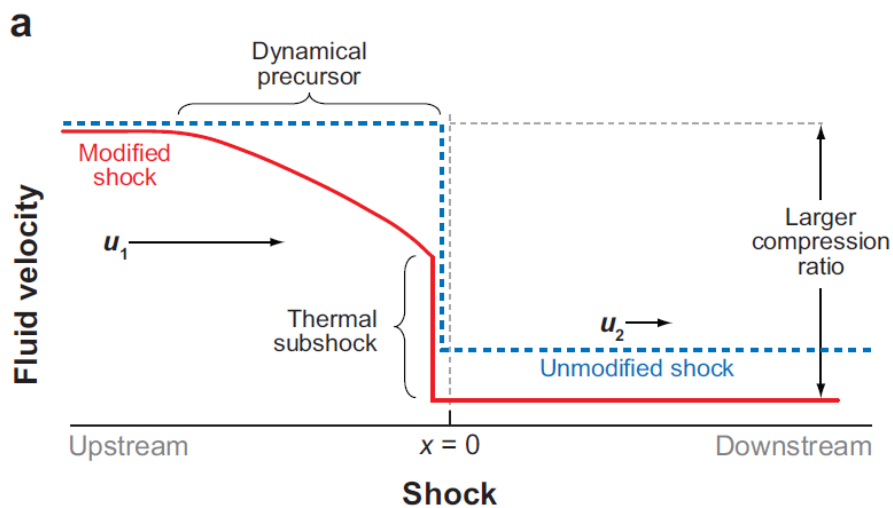
$$f(p) = A p^{-\alpha} + \alpha p^{-\alpha} \int_0^p p'^{\alpha-1} f_{-\infty}(p') dp'$$

注入激波加速粒子

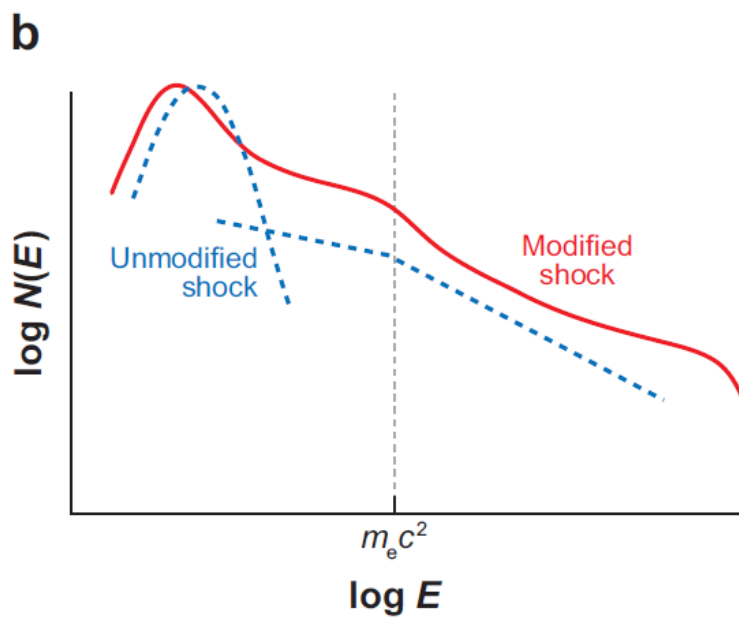
从激波上游对流

$$\alpha = \frac{3r}{r-1}$$

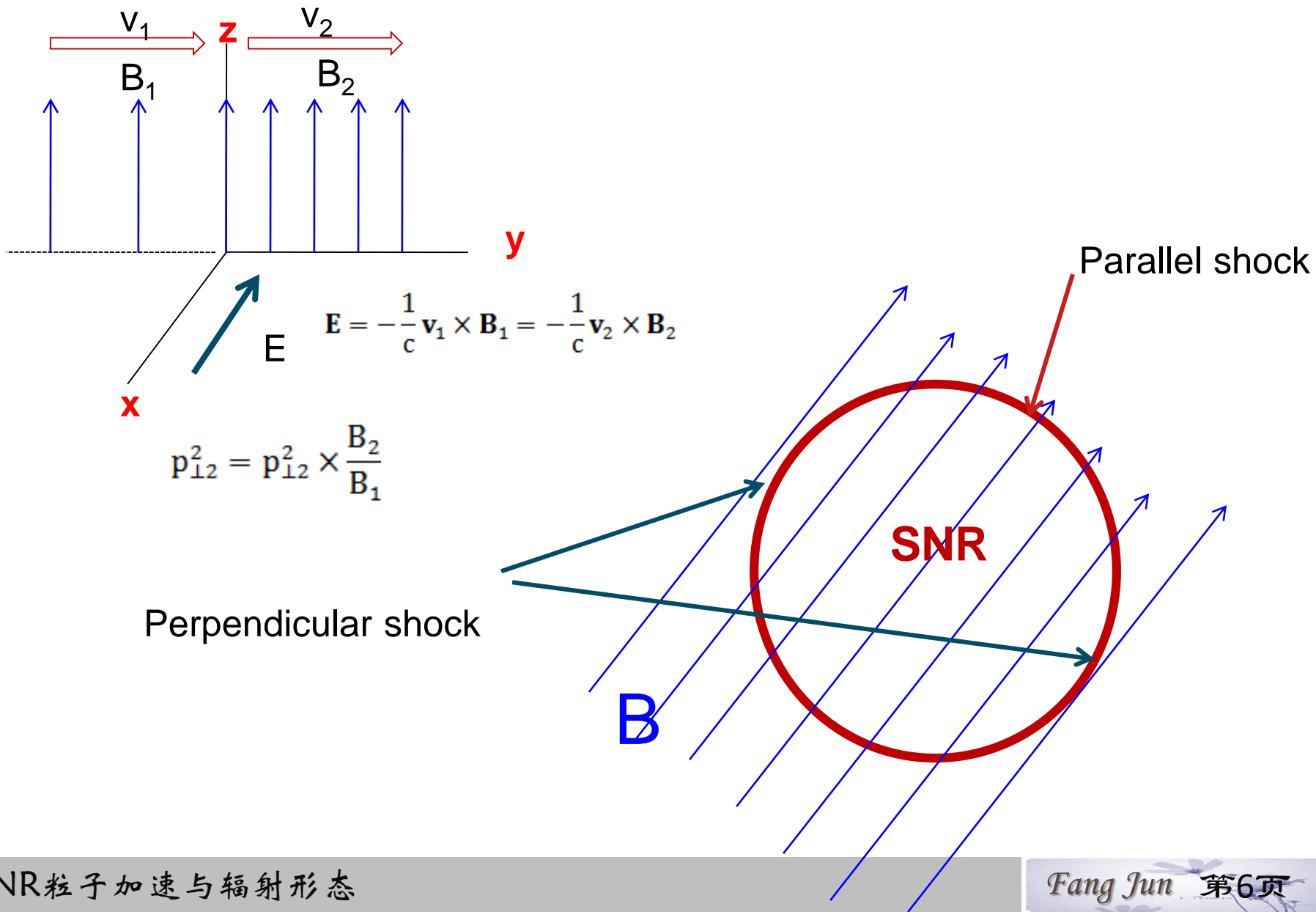
非线性效应



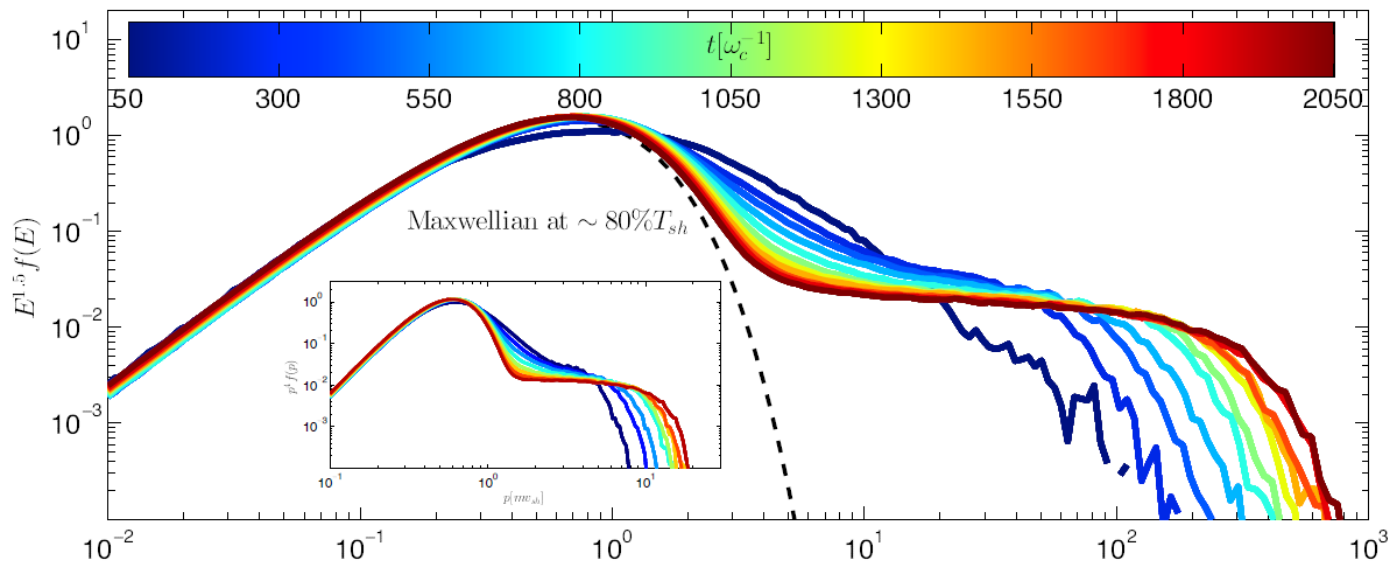
弯曲的粒子谱形
高能端变硬



(2) 激波漂移加速 (shock drift acceleration)



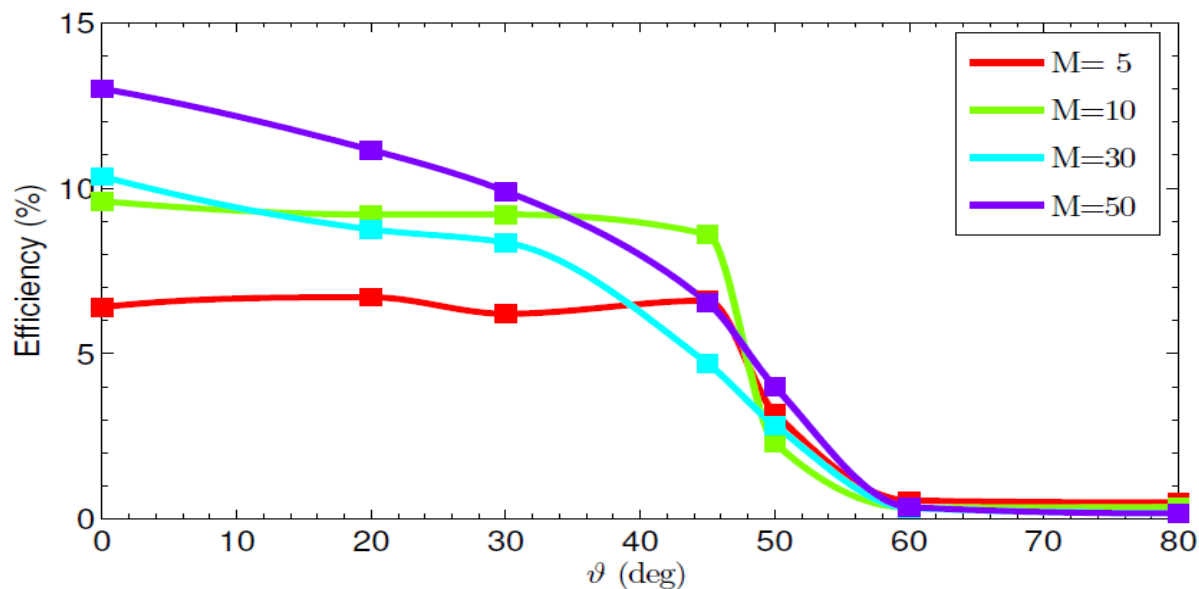
Hybrid simulation results Caprioli & Spitkovsky 2014



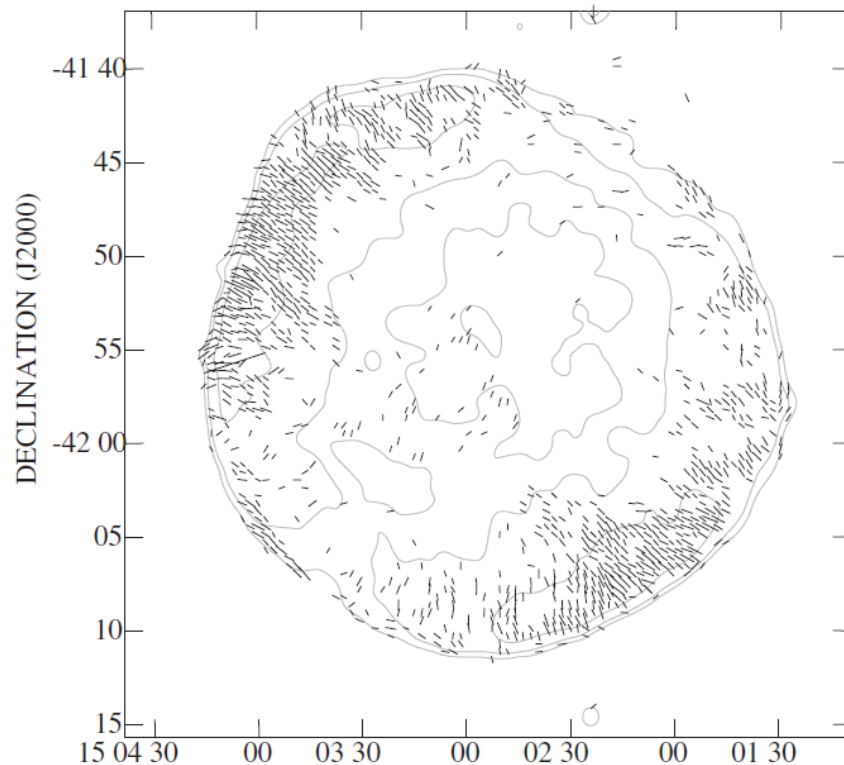
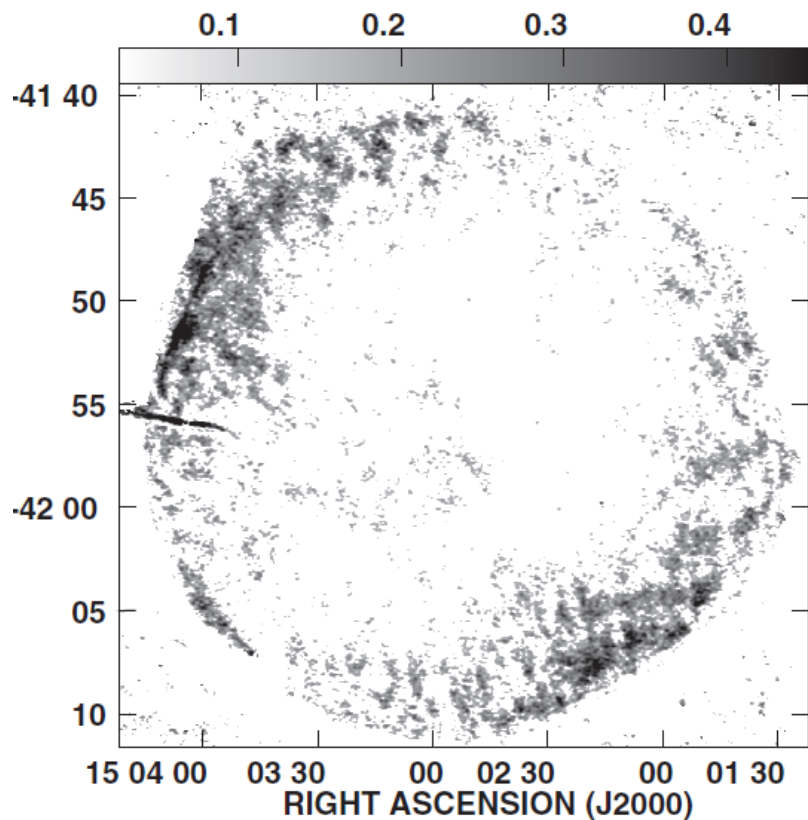
激波下游区离子随
能量分布

Maxwellian + power law

不同马赫数下的激波加速效率随 θ 变化，
 θ ：激波面法线与上游
磁场夹角



SN1006 射电偏振观测 Reynoso et al. (2013)



辐射符合极冠结构，辐射强的两极为平行激波。

辐射弱的两极对应垂直激波。

二、数值模拟结果

1、二维MHD 均匀环境

初始条件

抛射物质自由膨胀

$$\mathbf{v} = \mathbf{r}/t.$$

内部均匀，外部呈幂律分布

$$\rho_{ej}(t, r) = \begin{cases} \rho_c(t)(r/r_c)^{-n} & \text{if } r > r_c, \\ \rho_c(t) & \text{if } r < r_c. \end{cases}$$

星际介质分布均匀。假设有3/7的介质在外层，则有

$$r_c = R_{ej} \left[1 - \frac{x(3-n)M_{ej}}{4\pi\rho_0 R^3} \right]^{1/(3-n)}, \quad \rho_c = \frac{3(1-\eta)M_{ej}}{4\pi r_c^3},$$

$$\frac{\partial \rho}{\partial t} + \nabla \cdot (\rho \mathbf{v}) = 0, \quad (1)$$

$$\frac{\partial \rho v}{\partial t} + \nabla \cdot (\rho v v - B B) + \nabla P^* = 0, \quad (2)$$

$$\frac{\partial E}{\partial t} + \nabla \cdot [(E + P^*)\mathbf{v} - B(\mathbf{v} \cdot \mathbf{B})] = 0 \quad (3)$$

and

$$\frac{\partial \mathbf{B}}{\partial t} + \nabla \times (\mathbf{v} \times \mathbf{B}) = 0. \quad (4)$$

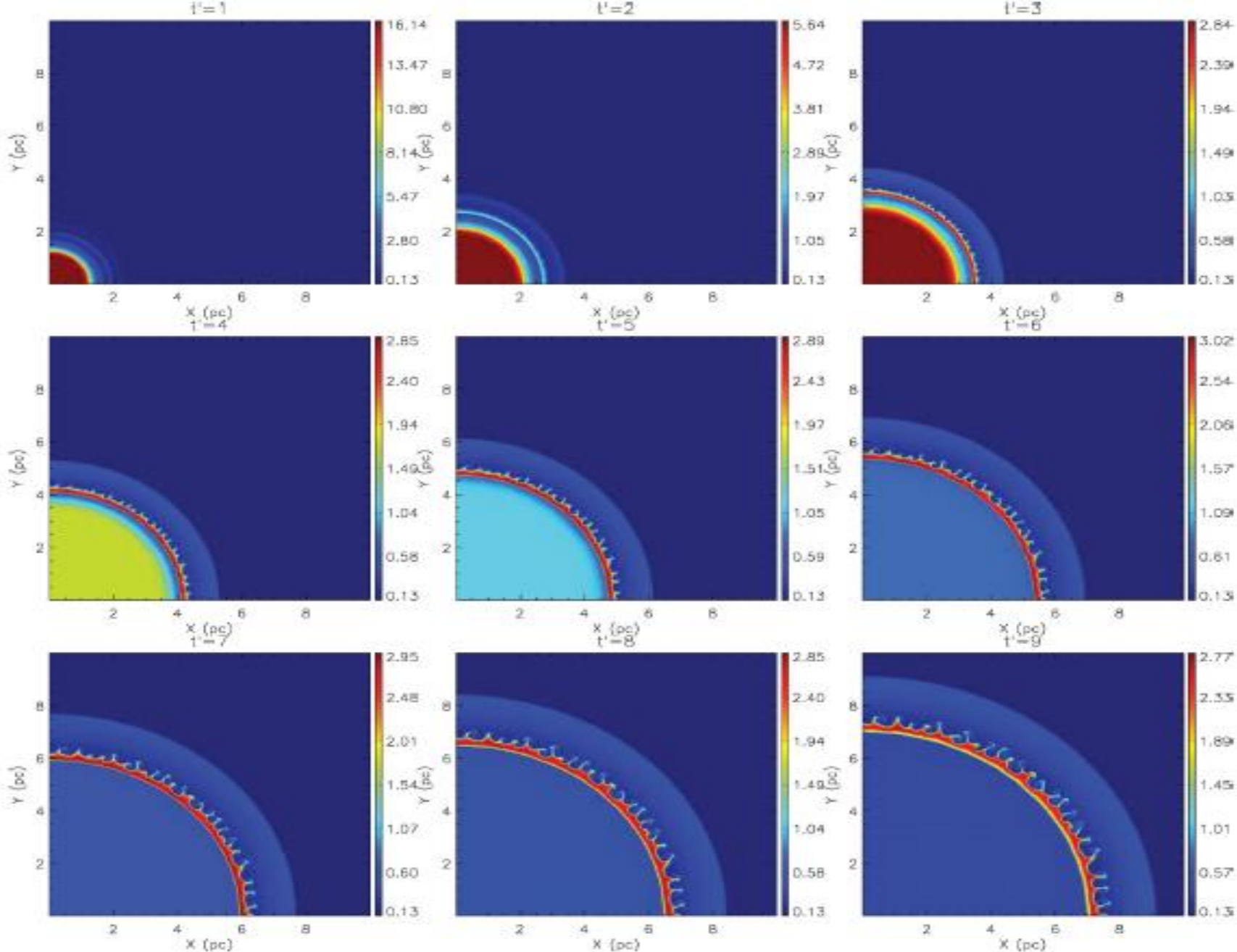


Figure 1. Spatial distribution of density in units of $m_{81} \text{ cm}^{-3}$ during the dynamical evolution of a SNR with $\gamma = 5/3$. Here, t' indicates the evolution time in units of 98 yr.

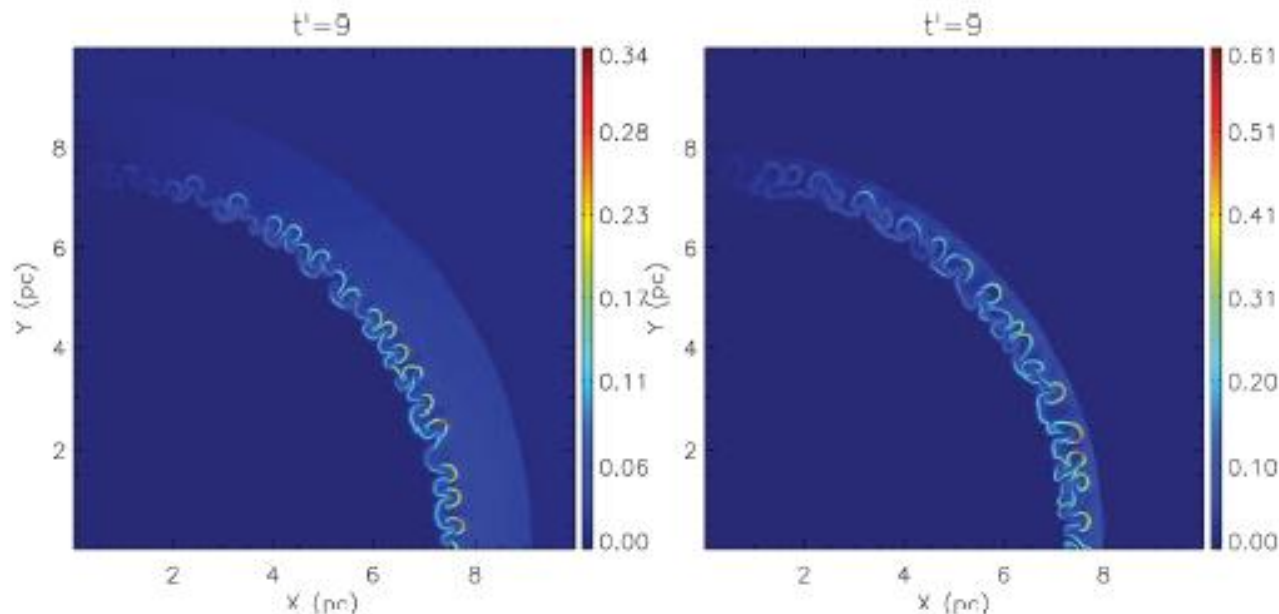


Figure 2. Left panel: magnitude of magnetic field in units of 4.586×10^{-4} G at $t' = 9$ for $\gamma = 5/3$; the other parameters are the same as Fig. 1. Right panel: magnitude of magnetic field in units of 4.586×10^{-4} G at $t' = 9$ for $\gamma = 1.2$; the other parameters are the same as Fig. 5.

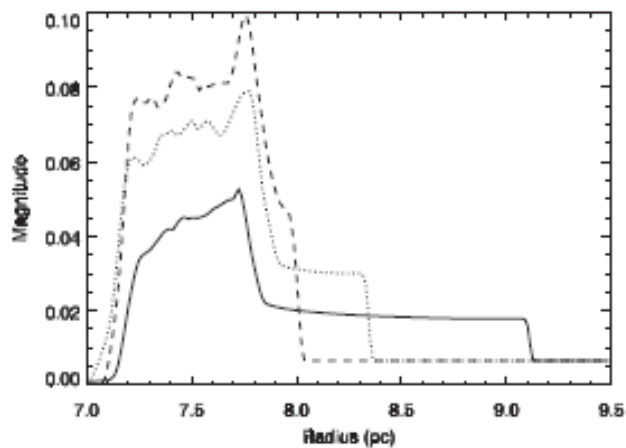


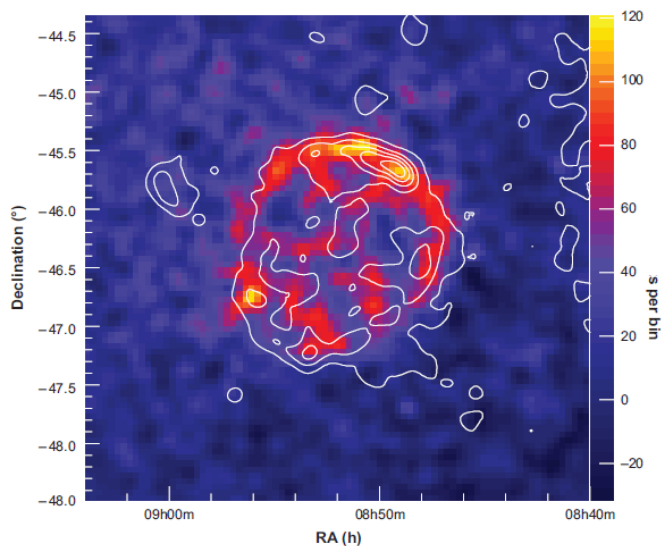
Figure 3. Angular-averaged magnitude of the magnetic field from the 2D simulations with $\gamma = 5/3$ (solid line), $4/3$ (dotted line) and 1.2 (dashed line). The other parameters are the same as Fig. 1.

激波加速及粒子逃逸过程可以改变有效绝热指数。绝热指数变小，激波压缩率增加，激波宽度减小。

激波区，被激波化的抛射物质遭遇激波化的星际介质，激发了Rayleigh-Taylor不稳定性，这些区域产生高密度和强磁场。

2、三维MHD 非均匀环境

RX J0852.0-4622



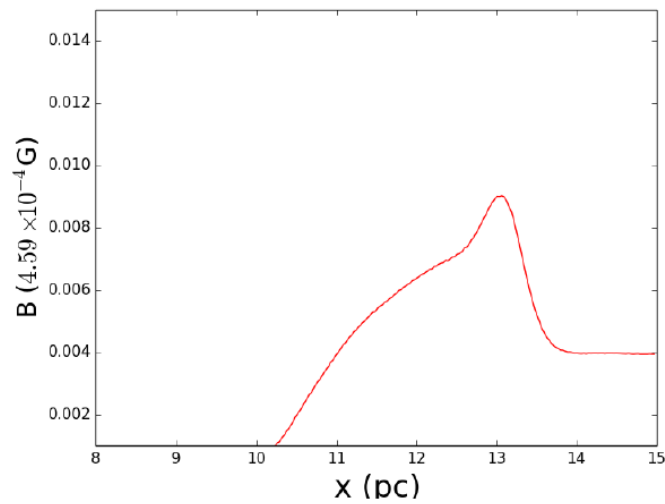
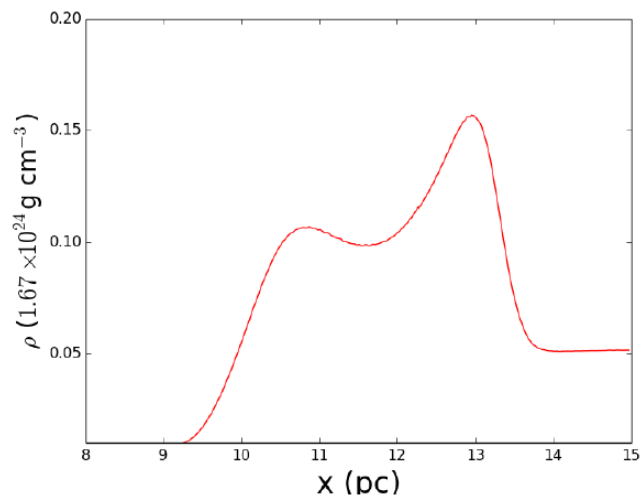
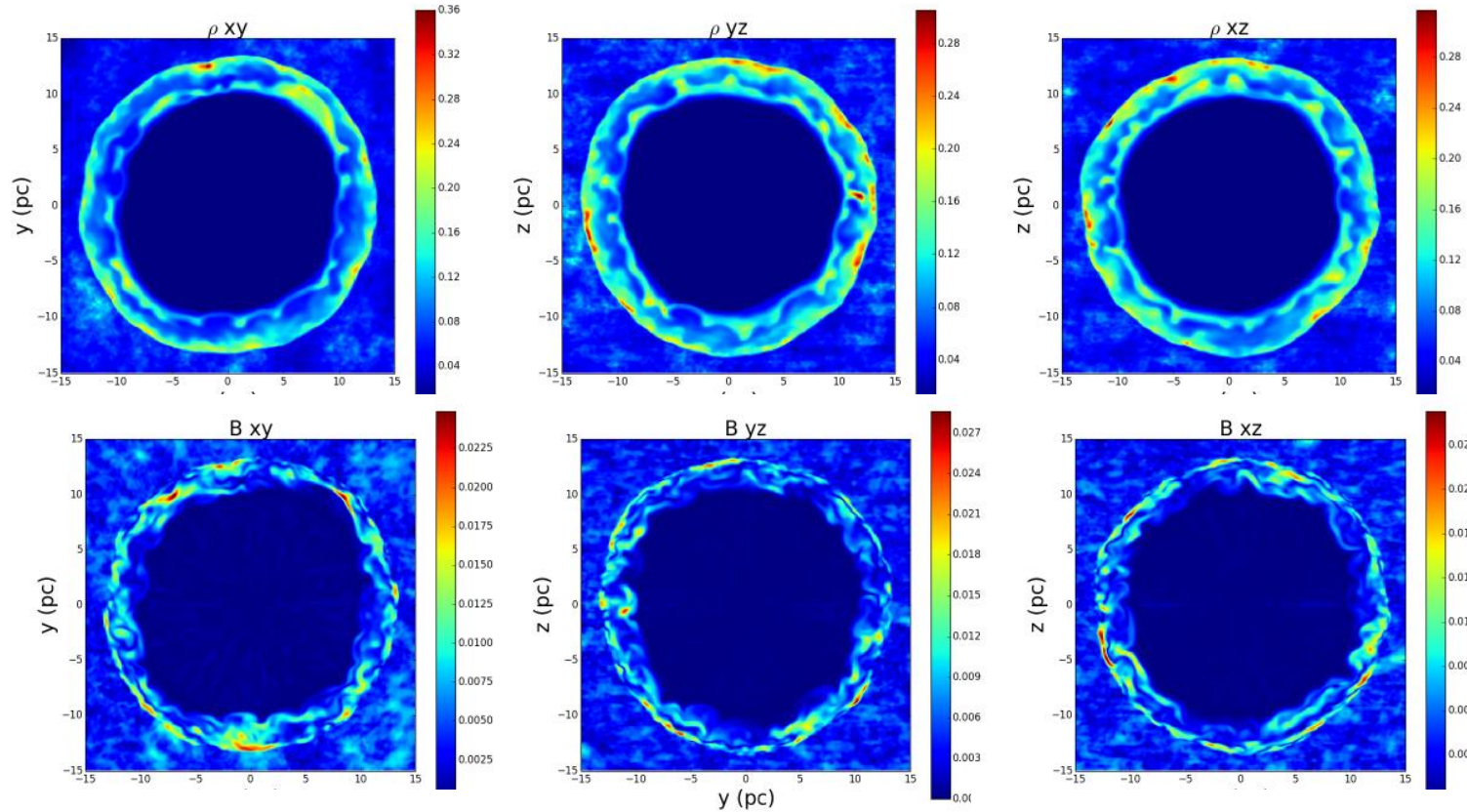
3D Kolmogorov-like power spectrum

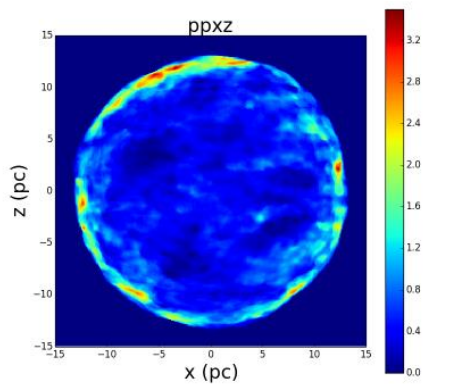
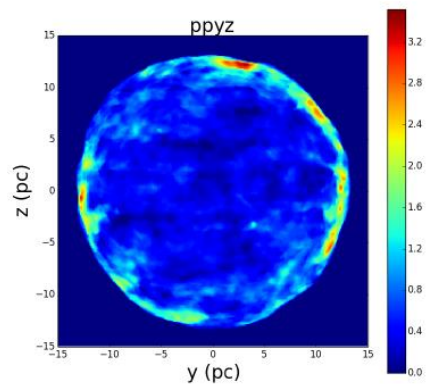
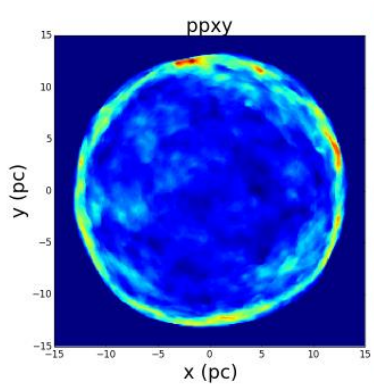
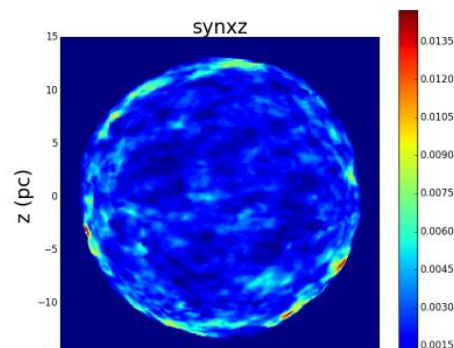
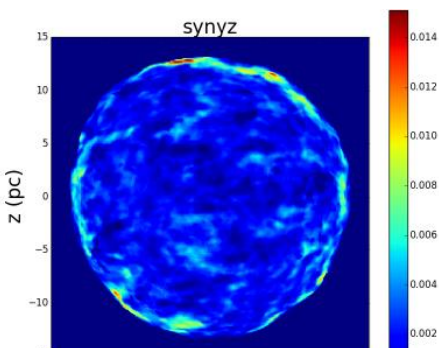
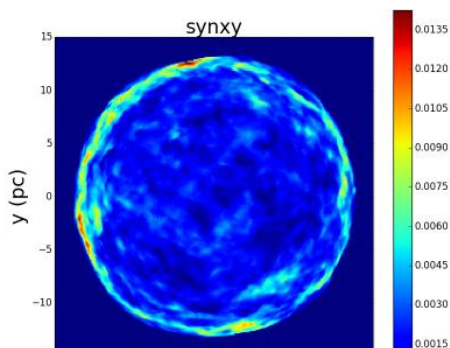
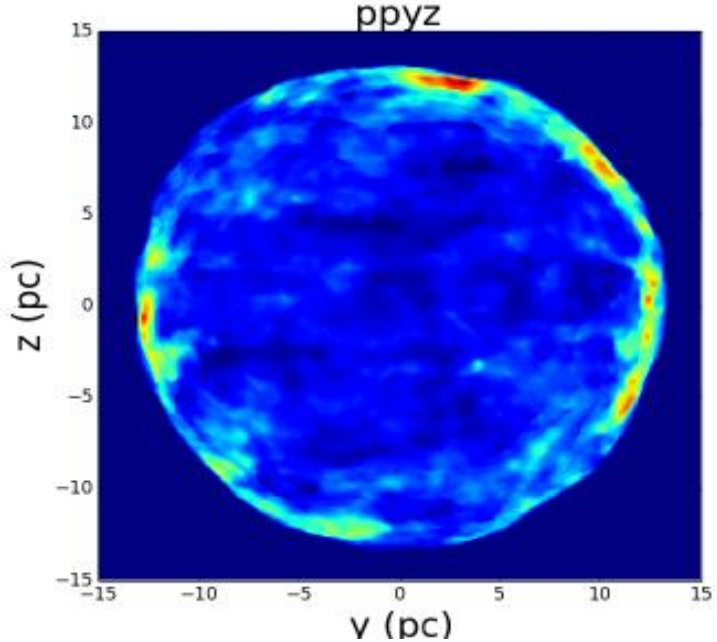
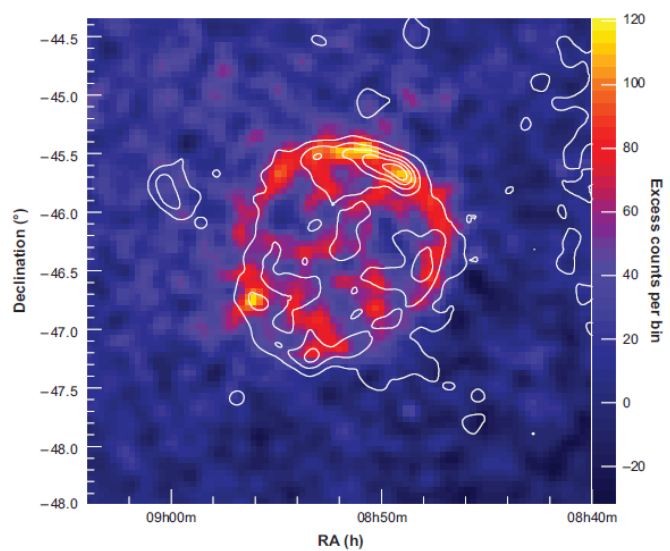
$$P \propto \frac{1}{1 + (kL_c)^{11/3}},$$

$$\mathbf{B}(x, y, z) = \mathbf{B}_0 + \delta\mathbf{B}(x, y, z),$$

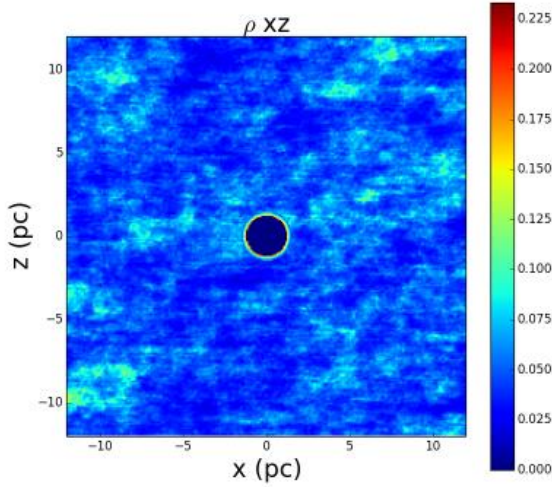
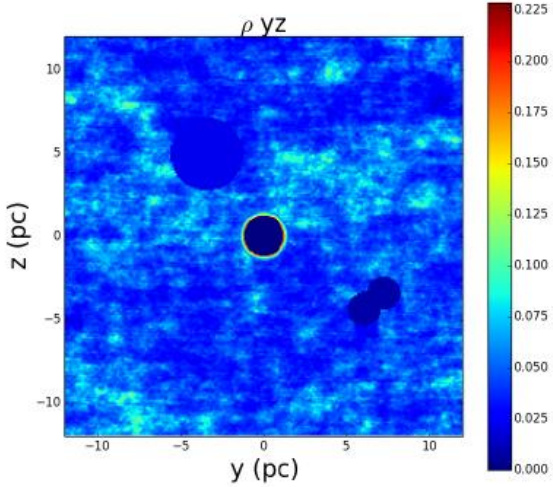
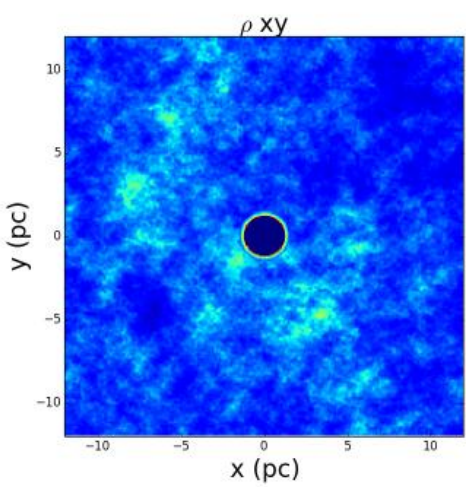
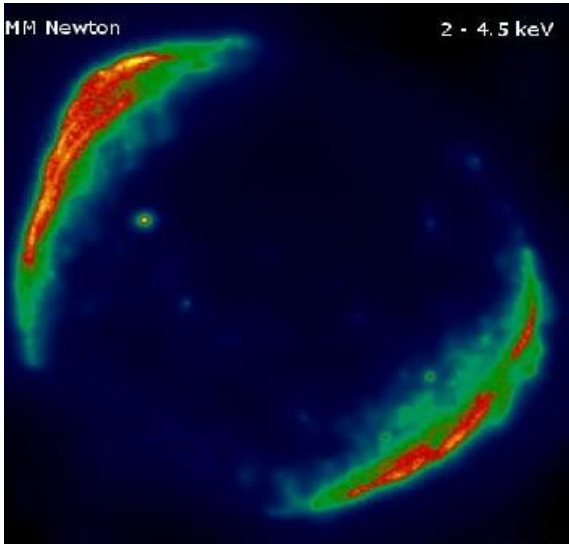
$$\delta\mathbf{B}(x, y, z) = \sum_{n=1}^{N_m} A(k_n) [\cos(\alpha_n)\hat{\mathbf{x}}'_n + i\sin(\alpha_n)\hat{\mathbf{y}}'_n] \exp(ik_n z'_n),$$

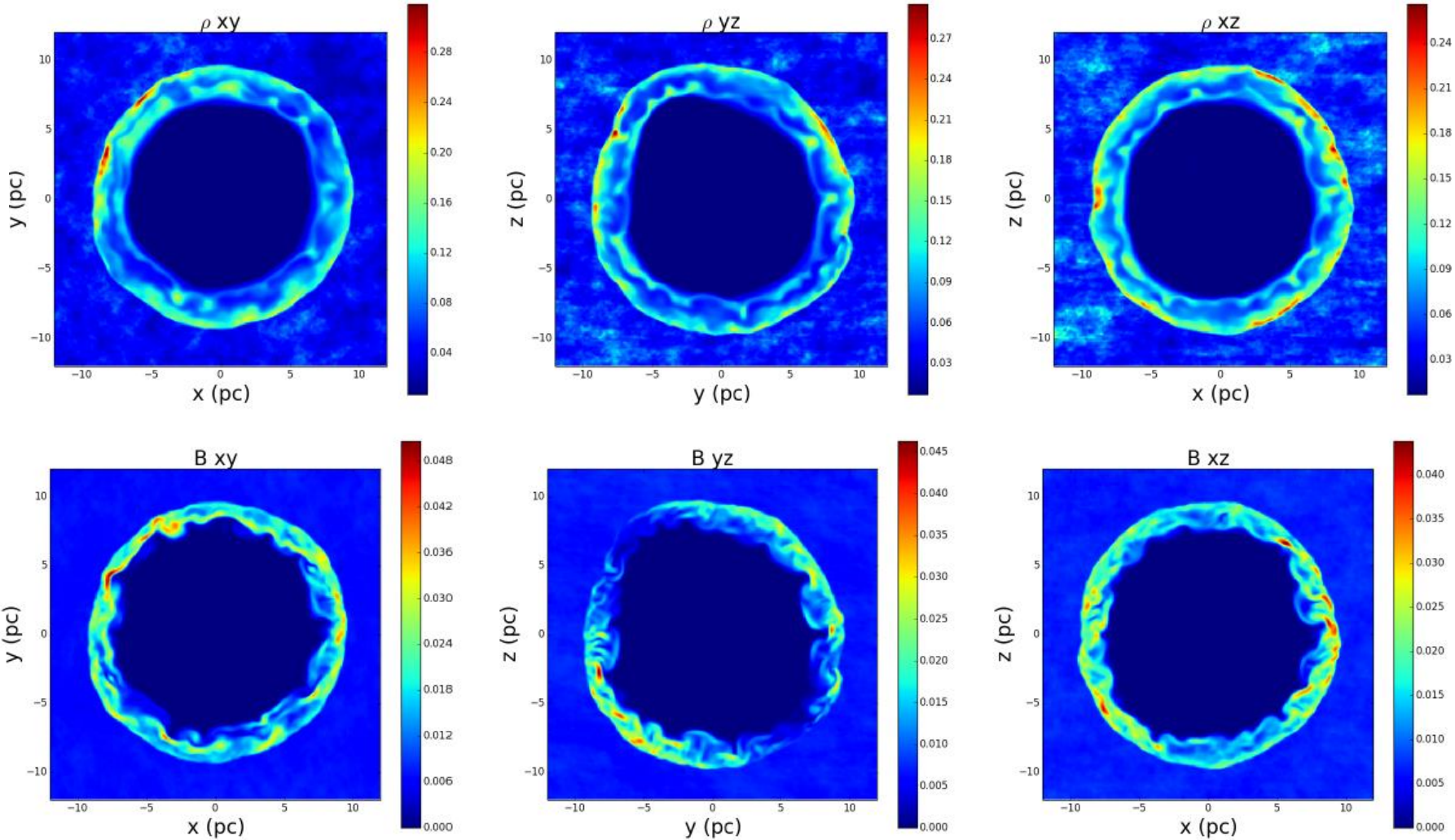
$$A^2(k_n) = \sigma_B^2 \frac{\Delta V_n}{1 + (k_n L_c)^{11/3}} \left[\sum_{n=1}^{N_m} \frac{\Delta V_n}{1 + (k_n L_c)^{11/3}} \right]^{-1},$$

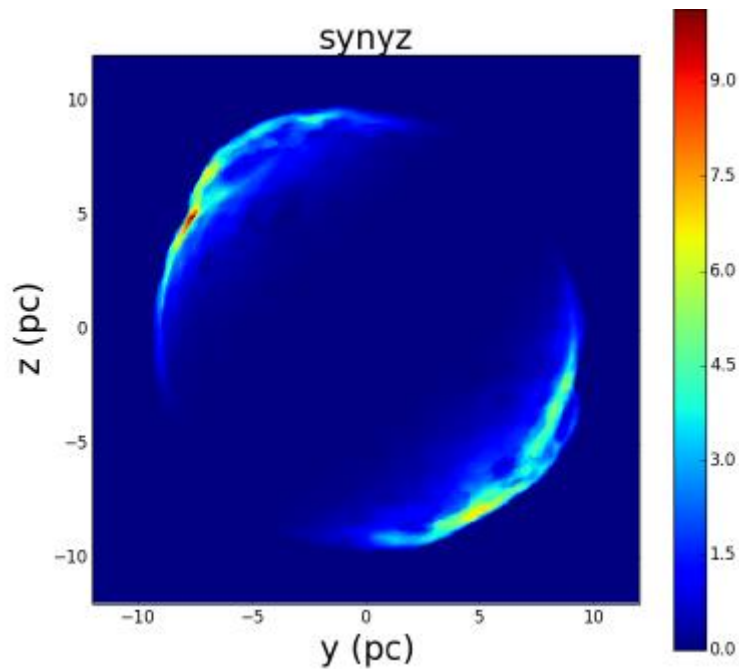
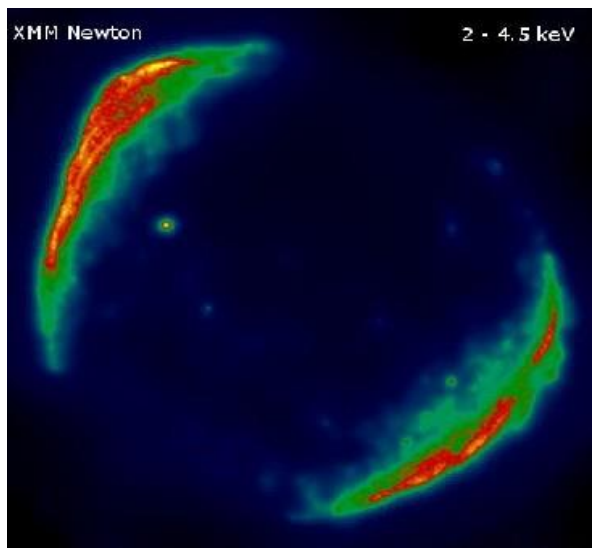
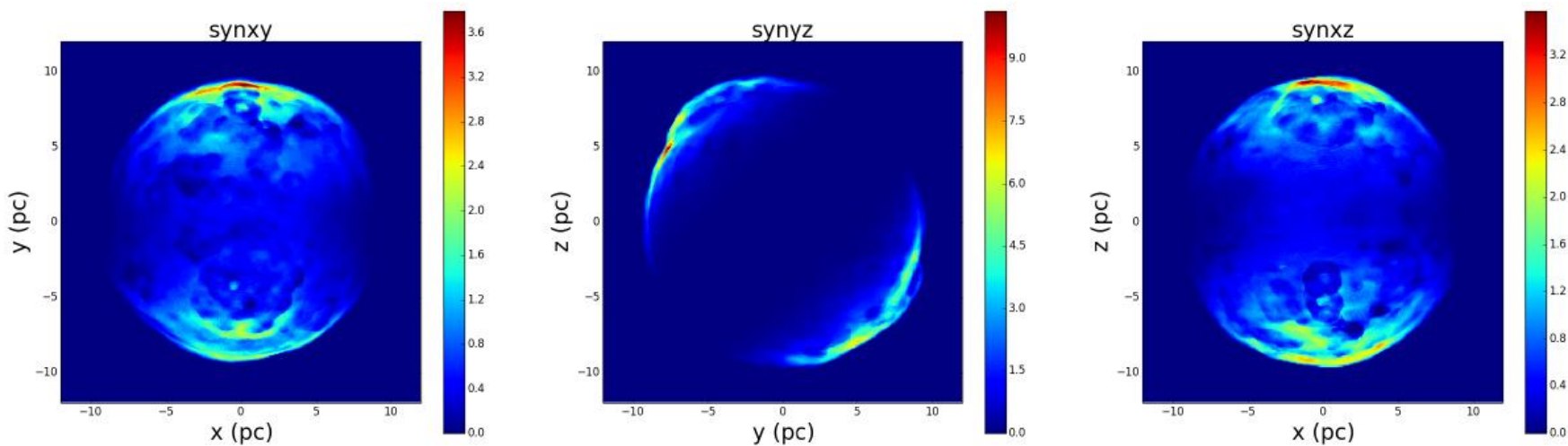




SN1006

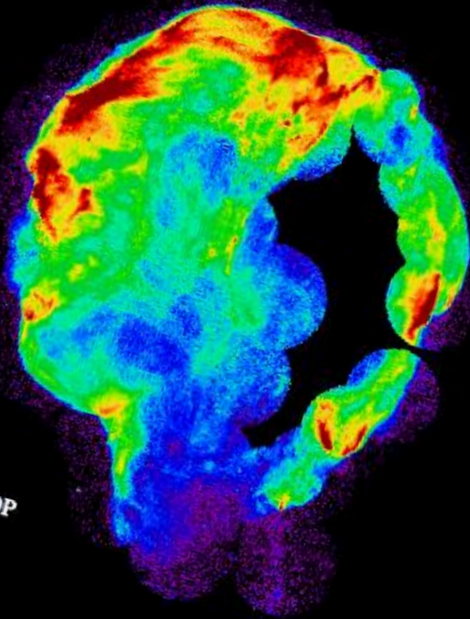






扩散激
波加速
假设

Cygnus loop



Bright X-ray source

limb brightened at X-ray and radio wavelengths

$d \sim 540 \text{ pc}$, $D \sim 28 \text{ pc}$, $T \sim 10^4 \text{ yr}$.

The remnant of a Type II SN explosion

a “breakout” region in the south,

a bright northern limb,

several depressions on the shock,

The profiles of the limbs on both sides of the

southern breakout are asymmetric.

There is a bright region within the outer limb in

the northwest.

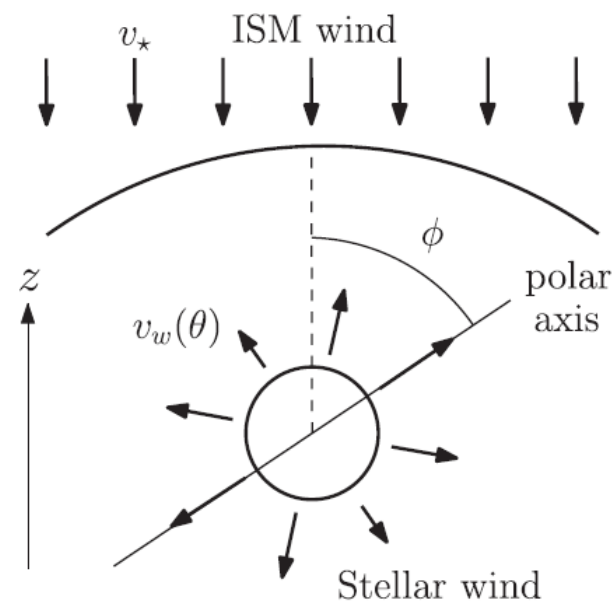
形态如何形成?

3D HD simulation

Assuming the SN is occurred in the cavity resulting from the interaction between the stellar wind of the progenitor with a spatial velocity and the ISM.

The density which increases from the equator towards the pole with an equator-to-pole ratio ξ .

$$\begin{aligned}\frac{\partial \rho}{\partial t} + \nabla \cdot (\rho \mathbf{v}) &= 0, \\ \frac{\partial \rho \mathbf{v}}{\partial t} + \nabla \cdot \rho \mathbf{v} \mathbf{v} + \nabla P &= 0, \\ \frac{\partial E}{\partial t} + \nabla \cdot (E + P) \mathbf{v} &= - \left(\frac{\rho}{m_{\text{H}}} \right)^2 \Lambda(T),\end{aligned}$$



$$\rho(r, \theta) = \frac{A}{r^2} f(\theta),$$

$$v_w(\theta) = \frac{v_p}{\sqrt{f(\theta)}},$$

星风演化

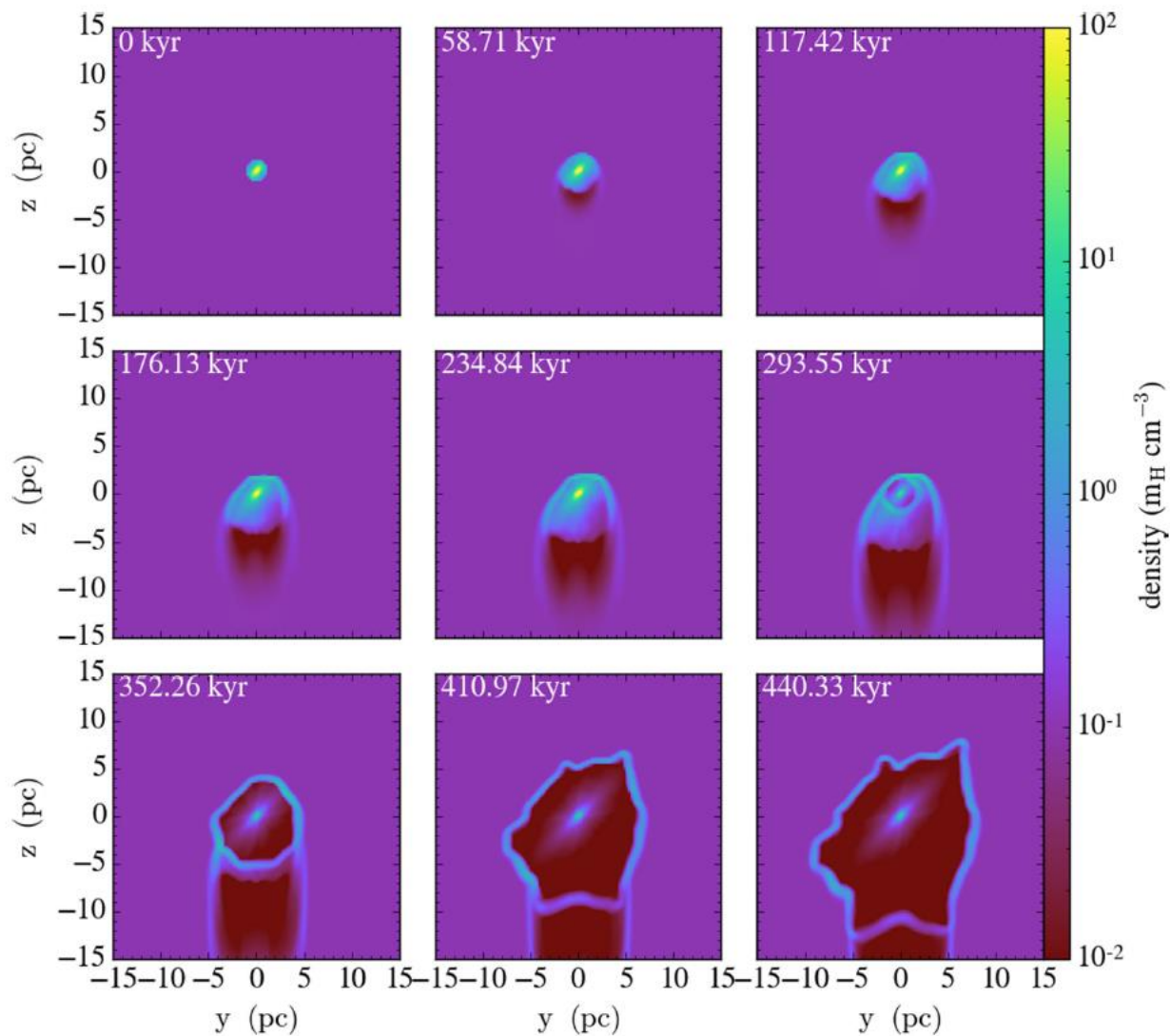
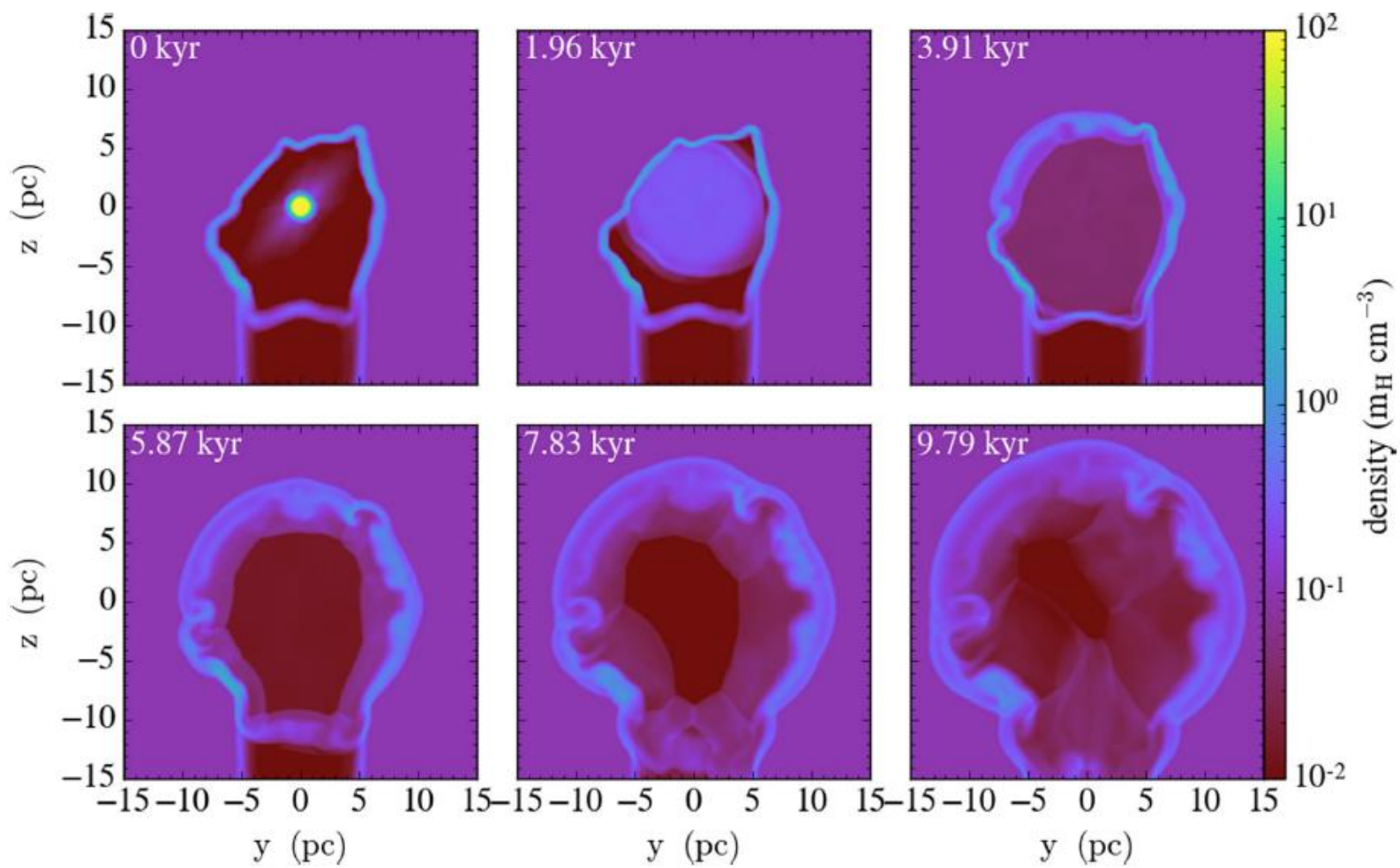
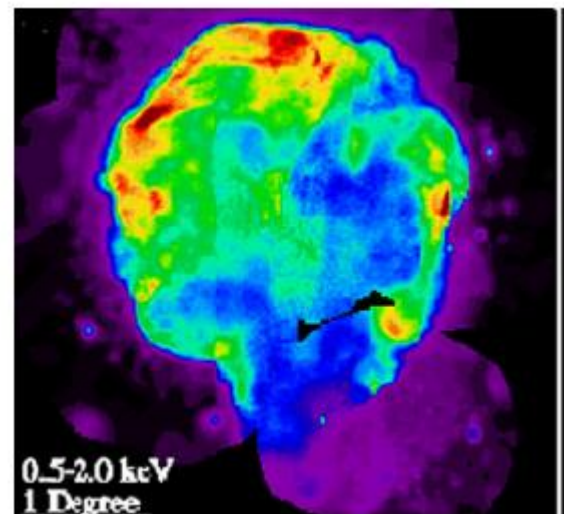
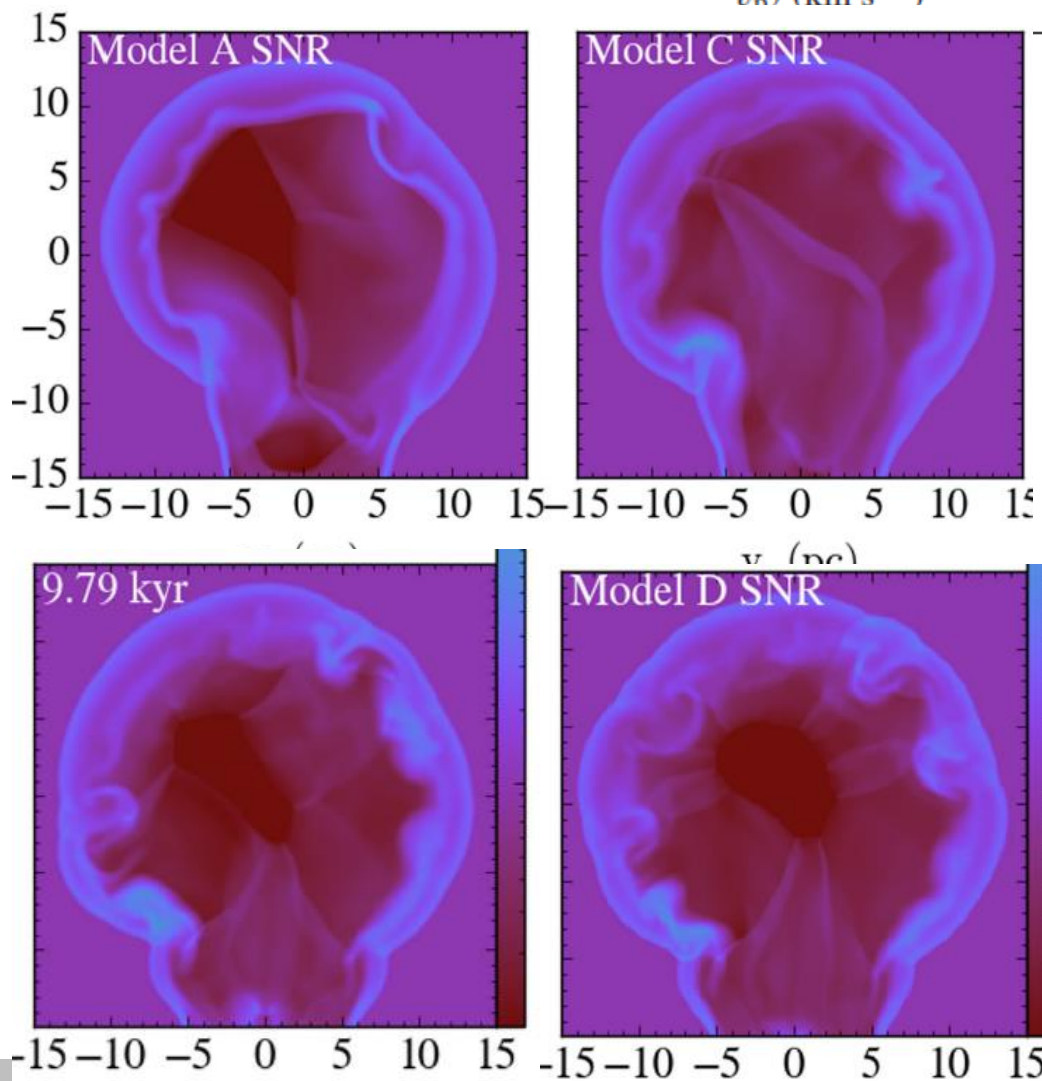


Figure 2. Evolution of the stellar wind for Model B. The yz slices of the mass density at $x = 0$ for different integration times are shown.



Parameter	Model A	Model B	Model C	Model D
α ($^\circ$)	50	50	50	30
ξ	10	10	10	4
v_{pl} (km s^{-1})	15	15	15	15
v_{∞} (km s^{-1})	15	300	150	300



Fang, Yu & Zhang 2017,
MNRAS, 464, 940

总结

- (1) 利用3D MHD数值模拟，研究在湍动环境下超新星遗迹的动力学演化过程；在加速粒子平行激波假设下，获得遗迹的辐射分布形态。
- (2) 超新星遗迹RX J0852.0-4622的非均匀辐射分布形态可解释为遗迹在湍动环境下演化的结果。
- (3) 通过假定存在低密度区域以及湍动环境，获得了遗迹SN1006的辐射形态。
- (4) 对Cygnus loop，假定遗迹在星风产生的空腔中演化。星风经历了速度不同两阶段，可产生观测到结构。

Thanks